

Characterization and structural analysis of RF magnetron sputtered strontium stannate thin films

Yusmar Palapa Wijaya¹, Khairul Anuar Mohamad², Abu Bakar Abdul Rahman³, Afishah Alias⁴,
Mohammad Syahmi Nordin⁵

^{1,2}Faculty of Electrical and Electronic Engineering, University Tun Hussein Onn, Johor, Malaysia

^{1,2}Microelectronics and Nanotechnology-Shamsuddin Research Centre, University Tun Hussein Onn, Johor, Malaysia

^{3,4}Faculty of Applied Sciences and Technology, Pagoh Campus, University Tun Hussein Onn, Johor, Malaysia

⁵School of Computer Science and Electronic Engineering, University of Essex, Colchester, United Kingdom

Article Info

Article history:

Received Jul 28, 2020

Revised Jan 7, 2021

Accepted Jan 20, 2021

Keywords:

Perovskite

RF magnetron sputtering

SrSnO₃

Strontium Stannate

Thin Film

ABSTRACT

This paper presents physical and morphology properties of strontium stannate (SrSnO₃) perovskite-type as a candidate of an n-type material thin film for organic-inorganic hybrid diode heterojunction for optoelectronics application. Typical wet-process of SrSnO₃ deposition produce thick film and having 10⁻⁸ S/cm order in conductivity. The SrSnO₃ thin films were deposited on ITO glass substrates by RF magnetron sputtering using a purity 99.9% SrSnO₃ target with 5.0 mTorr of gas pressure and 100 W of RF power at room temperature. The gas composition of pure argon (75%) and reactive oxygen gas (25%) was used for 60 min. XRD diffraction patterns revealed that the thin films are orthorhombic crystal structure with lattice parameter a=5.7040 Å, b=8.06 Å and c=5.7080 Å with a strong orientation in the (002) direction. SEM images showed that films exhibited uniform surface morphology with a roughness average of R_a=2.258 nm and thickness of 311 nm. The EDX spectrum confirmed the presence of O, Sr, and Sn elements in the films with 75.22%, 8.29%, 16.49% in atomic number, respectively. The films were having a conductivity of 8.33×10² S/cm with low resistivity of 12.4×10⁻³ Ω-cm.

This is an open access article under the [CC BY-SA](https://creativecommons.org/licenses/by-sa/4.0/) license.



Corresponding Author:

Yusmar Palapa Wijaya

Faculty of Electrical and Electronic Engineering

University Tun Hussein Onn

86400, Parit Raja, Batu Pahat, Johor, Malaysia

Email: yusmar.wijaya@gmail.com

1. INTRODUCTION

In recent years, the organic-inorganic pn junction has been increasing attention in research communities of photovoltaics and light-emitting diodes. In many demonstrations, a particular type of perovskite has shown improvement compared to crystalline Si and III-V as a photodetector material [1]. Performance of perovskite that absorbs light effectively in the broadband range with photo-generation yield improvement and high charge carrier mobility, a combination that provides a promising potential for exploiting sensitive and fast photodetectors that are targeted for image sensing, optical communication, environmental monitoring, chemical or biological detection [2], [3]. There are semiconductor devices that detect an optical signal such as photodiode, photoconductor and photo-field effect transistor (FET) [4]. Perovskite such as strontium stannate (SrSnO₃) also reported having good photoluminescence and photocatalyst properties [5]. According to its valence band and conduction band condition, the SrSnO₃ thin films has possibility to split

water into hydrogen and oxygen [6]. The large band gap of this semiconductor (~ 4.1 eV) desirable for the optoelectronic device at short wavelength [6]. In the development of organic-inorganic p-n junction based on SrSnO_3 , the synthesization of SrSnO_3 as n-type paired with organic p-polyaniline (p-PANI) by Faisal *et al.* and a combination of organic p-type reduced graphene oxide (rGO) with SrSnO_3 by Venkatesh *et al.* as a nanocomposite used to enhance photocatalytic activity [7], [8].

The stannate based perovskite-type materials have a general formula of ASnO_3 by group alkaline-earth stannate for A molecule that are Ba, Sr, or Ca with the ionic radius of 135 pm, 118 pm and 100 pm, respectively [5]. ASnO_3 has a wide application such as new chemical sensor, stable capacitor, flat panel display and humidity sensor [9]. As stated in other papers, strontium stannate has achieved charge mobility of $18.5 \text{ cm}^2\text{V}^{-1}\text{s}^{-1}$ by Ta doping using pulsed laser deposition (PLD) technique [10]. Strontium stannate is perovskite type material which is classified as n-type semiconductor due to oxygen vacancy [11], [12]. Synthesis of SrSnO_3 has been reported by many researchers that the development of thin films from powder using a chemical deposition technique through hydrothermal, sol-gel and solid-state ratio [13]. In a wet-process technique, the thin films show a thickness range of several micrometers. As a thick film, it exhibits low conductivity values of order 10^{-8} S/cm. However, there are few researchers reported on the deposition of SrSnO_3 using dry-processes such as a sputtering deposition. Wakana *et al.* have deposited strontium material to magnesium oxide (MgO) substrate by an 50-W RF sputtering technique at a gas pressure of 80 mTorr with a gas composition 50% of pure argon and 50% of oxygen. The target position was set perpendicular (90°) to the surface substrate [14]. Although a PLD technique has been used to deposit doped SrSnO_3 thin films onto a strontium titanate crystal (STO) substrate [10], preparation and fabrication of SrSnO_3 thin films have not been reported by a sputtering deposition on glass substrates. In this paper, we report the preparation and deposition of a transparent and conductive SrSnO_3 thin films by an RF magnetron sputtering onto an ITO coated glass substrate at room temperature. The structure, surface morphology and electrical conductivity were systematically investigated to reveal its potential for optoelectronics applications.

2. RESEARCH METHOD

Figure 1 shows a flowchart of fabrication and deposition of SrSnO_3 film on ITO coated glass substrate using an RF magnetron sputtering technique. The preparation of sample starts the process by cleaning using ultra-bath, then load it into sputtering chamber. In the following steps, the setting of parameters required should be adjusted and process of deposition will be activated.

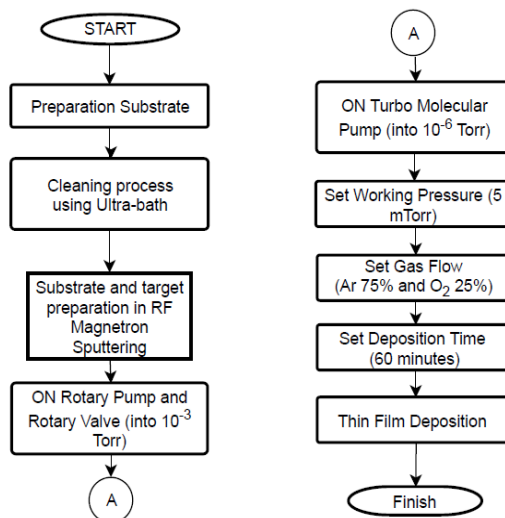


Figure 1. Flowchart of fabrication and deposition of SrSnO_3 thin film

2.1. Substrate Preparation

Indium tin oxide ($\text{In}_2\text{O}_3:\text{Sn}$) known as ITO coated glass was used as a substrate with a dimension of $2 \times 2 \text{ cm}^2$. The substrates were cleaned using acetone, methanol, and de-ionized water with sonication for 15 min each [15]. After the sonication process, the substrates were dried in a oven for 10 min at a temperature of

70 °C. This process is essential to ensure the substrate surface clean from any impurities that correlated to its contact quality.

2.2. Deposition of thin film

Figure 2 depicts schematic of sputtering chamber and its components. The pre-sputtering technique has been used to ensure the substrates was free from any oxide layers during 15 minutes. There are two types of power source for sputtering in common, namely as direct current (DC) and radio frequency (RF). RF power source often assigned to achieve a smoother growing result on the surface of a thin film [16]. In this experiment, deposition condition was set up using a 100-W RF power source, an operating frequency of 1365 Hz, a chamber base pressure of 7.7×10^{-6} Torr and gas pressure of 5 mTorr. Pure argon was used as sputter gas and oxygen as reactive gas by composition 75% and 25%, respectively [17]. Distance between target and substrate is about 120 mm non-perpendicular and a deposition time of 60 min. Strontium stannate disc with purity 99.9%, 3-inch in diameter and 0.125-inch in thickness (Plasmaterials) is used as a sputter target. From two cathodes available in the sputtering chamber, only one cathode was chosen to connect with RF power source, and its angle of the target to the base is 45° as depicted in Figure 2.

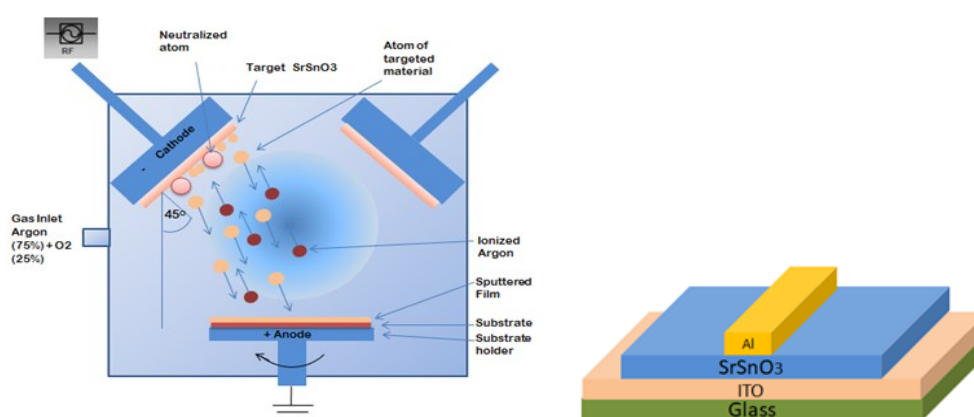


Figure 2. RF magnetron sputtering process and structure of thin film

For electrical conductivity, aluminium (Al) was used as a metal contact for the SrSnO₃ thin films using thermal evaporation technique. Al wire was placed inside the bottom of an evaporation chamber in a tungsten boat. The boat initially was heated up and increase the temperature by increasing the current until Al inside reach the melting point at a large current of 39 A with a small voltage. The evaporation time was set for 25 min.

2.3. Measurement and characterization

X-ray diffraction (XRD) measurement was deployed to analyze the structure of the material. XRD is the non-destructive technique and used widely for structural analysis. It can be used to investigate structural quantities such as lattice parameters of crystals, strain state, crystalline orientation, layer thickness and chemical composition of alloy [18]. Meanwhile, The surface morphologies were observed by atomic force microscope (AFM), and the perpendicular surface area characteristic was investigated by a field-emission scanning electron microscope (FESEM) [19]. The scanning electrons interact with atoms on surface producing signals of surface topography. Besides, energy dispersive X-ray spectroscopy (EDX) was set up to obtain material composition [20]. Lastly, the contact angle measurement was used to assess wettability, horizontal, smooth, homogenous and massive solid system.

3. RESULTS AND DISCUSSION

3.1. Thin film characteristics

Figure 3 shows the SEM image of the cross-section of SrSnO₃ thin film. As depicted in Figure 3 (b), SrSnO₃ thickness at observed length image area has even depth, approaching 310 nm. For 60 minutes of the process duration, it results in 311-nm of thickness over 203-nm thick of ITO film which measured by SEM cross-section and its deposition rate reaches ± 5.18 nm per min. Thus, the deposition time affects the atomic number deposited into the substrate in bulk type.

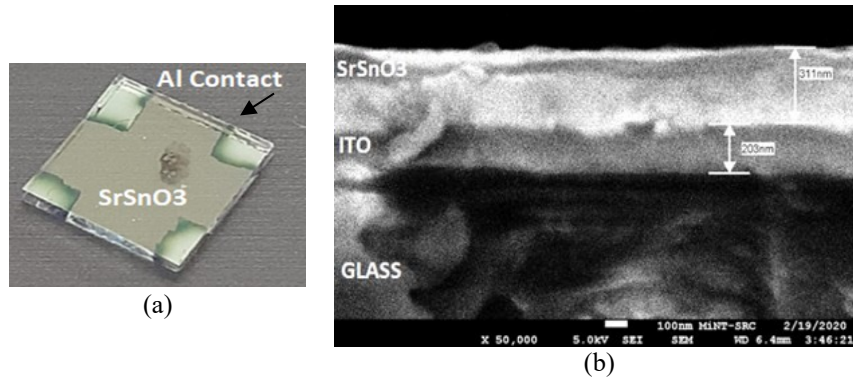


Figure 3. These figures are: (a) deposition of SrSnO₃ thin film, (b) cross-section of SEM image for thickness measurement (50000x, 5kV) on a ITO-coated glass substrate

Figure 4 presents the XRD patterns of SrSnO₃ thin film using Cu K α radiation ($\lambda = 0.1546$ nm). The patterns of two samples indicated a similar strong orientation in the (002) direction. The SrSnO₃ is the orthorhombic perovskite crystal structure, and its interplanar spacing can be calculated using the following formula:

$$\frac{1}{d^2} = \frac{h^2}{a^2} + \frac{k^2}{b^2} + \frac{l^2}{c^2} \quad (1)$$

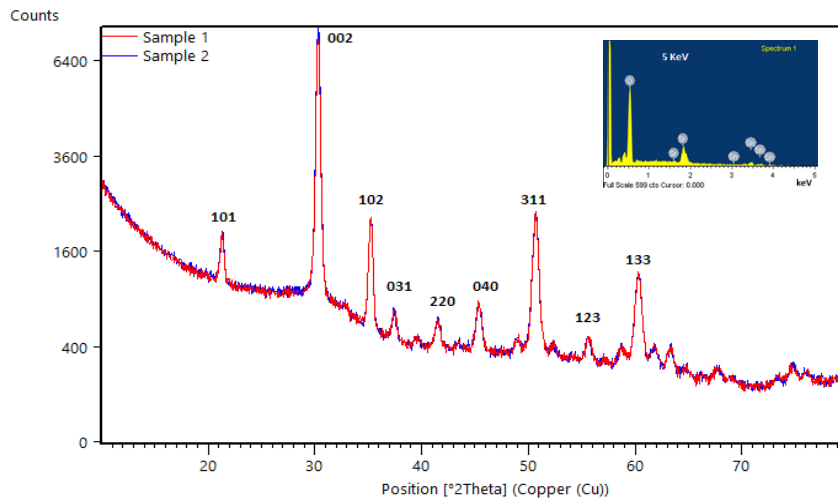


Figure 4. XRD pattern of an RF magnetron sputtered SrSnO₃ thin films. The inset shows the SEM-EDX results

where d is interplanar spacing, hkl represents the plane orientation and abc represents the lattice length. Thus, the value of $d = 0.294$ nm was obtained. To inspect the crystallinity, it is necessary to measure full-width half maximum (FWHM) of the diffraction pattern. The FWHM of (002) diffraction as the highest intensity is 0.472, and its crystallite size structure showed a delta of $2\theta < 1^\circ$. Table 1 summarizes the peaks position and crystal characteristics of the SrSnO₃ thin film.

Table 1. Peaks position and its crystal characteristic

Peak No.	Pos ^o [2 θ]	FWHM	(hkl)	Crystallite Size (Å)
1	30.357	0.472	002	177
2	35.25	0.289	102	297
3	52.411	0.472	311	191

Residual stress has shifted peaks in one and other directions which are correlated with balance stress at grain boundaries and satisfy constraints on the strain tensor [21]. It shows orthorhombic crystal structure with lattice parameter $a = 5.7040 \text{ \AA}$, $b = 8.06 \text{ \AA}$ and $c = 5.7080 \text{ \AA}$ ($a \neq b \neq c$). The angles between the lattice $\alpha = \beta = \gamma = 90^\circ$, perpendicular each other. The value of lattice almost similar as reported by Mary C.F. Alves *et al.*, which provide lattice data for temperature treatment to SrSnO_3 thin film with $a = 8.07274 \text{ \AA}$, $b = 5.71122 \text{ \AA}$ and $c = 5.71251 \text{ \AA}$ based on Rietveld refinement [22]. It is indicating that the crystal lattice perspective led to an interchange of lattice data value. Crystallite size can be measured use Scherer's equation involving Bragg angle in the structure [23].

The EDX spectral revealed the presence of elements and composition percentage with contains of O (30.96%), Sr (18.69%), Sn (50.35%) in weight and 75.22%, 8.29%, 16.49% in atomic number, respectively, using EDX apparatus with 5-keV power. However, this result is slightly different with its database with the percentage for the weight of O (18.073%), Sr (34.45%), Sn (46.67%) and its atomic number of 57.14%, 30.15%, 12.69%, respectively. The samples have a larger percentage number for oxygen (O) and tin (Sn) compared to a database, which it could be caused by a exposure of EDX beam reaching ITO layer which consist two elements above.

Figure 5 shows three-dimensional (3D) surface morphologies of the SrSnO_3 thin films deposited on ITO coated glass using a 100-W RF magnetron sputtering. These images indicated that the uniformity of the deposited atoms was achieved. As a solid material surface, it also indicates massive bombardment of ion from target to the rotating substrate.

Figure 6 shows the roughness average (R_a) and the grain size of SrSnO_3 thin films based on an area ranging from 1000 to 5000 nm^2 . As shown in Figure 6, linear trends showed between the surface roughness and the grain size. At area 5000 nm^2 , it results in a $R_a = 2.258 \text{ nm}$ and a grain size = 197.2 nm, which indicated a uniform surface. The value of R_a may be affected by the 100-W RF power condition, and the axis of the sputtering target of 45° as thin film deposited with perpendicular axis generates smoother roughness ($< 1 \text{ nm}$) [14].

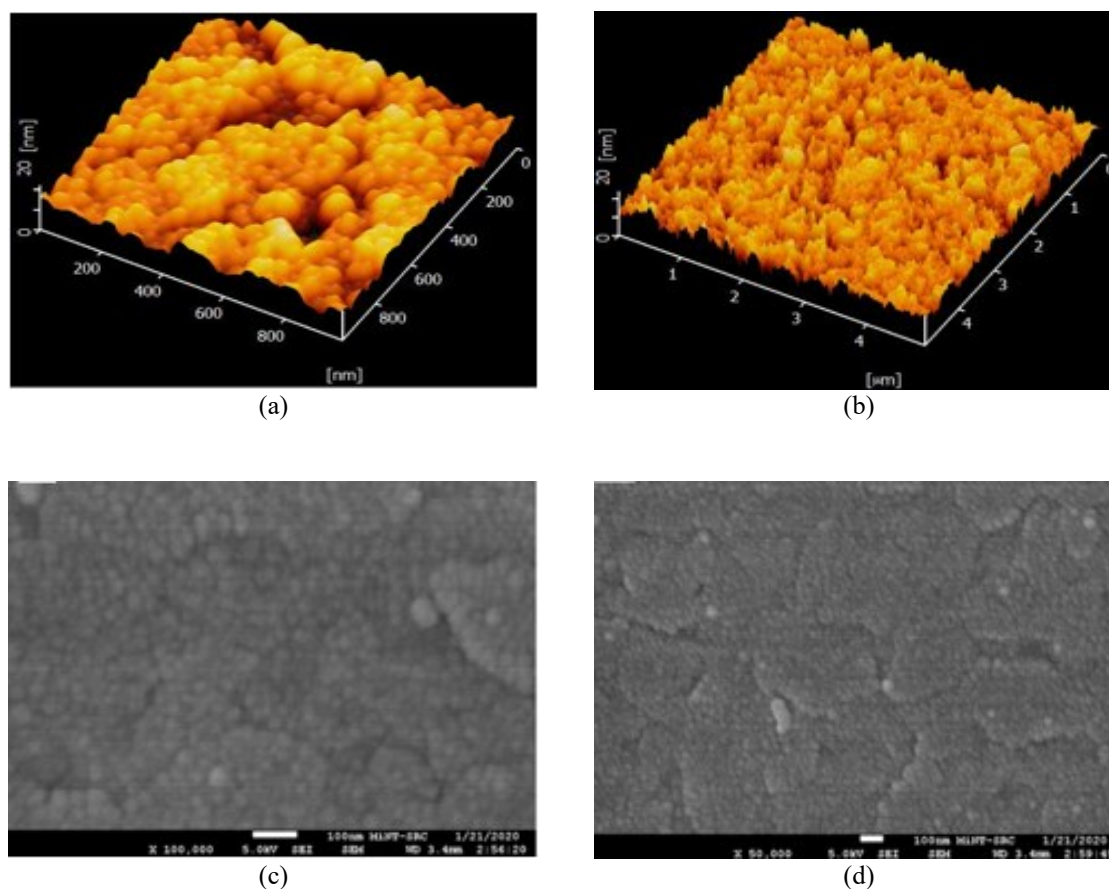


Figure 5. AFM images of: (a) area $1 \times 1 \mu\text{m}^2$, (b) area $5 \times 5 \mu\text{m}^2$ with respective SEM images of, (c) 100.000x magnification, (d) 50.000x magnification

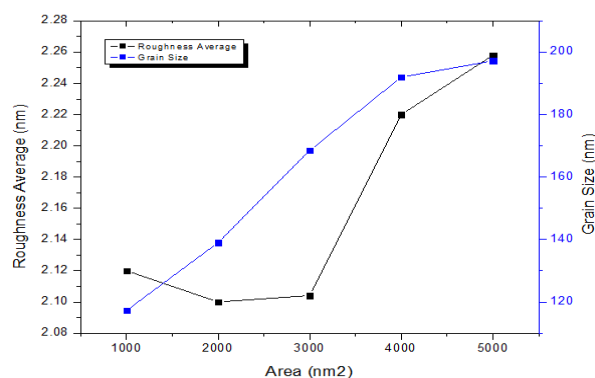


Figure 6. Roughness average (R_a) and grain size of SrSnO_3 thin film

Smooth roughness of the surface can be achieved by adjusting power lower than 100 W, as mentioned by other researchers [24]. In chemical synthesis growth mechanism, uniform and regular shape in the form of nanorod developed [13]. Based on RF magnetron sputtering deposition process, Wakana *et al.* has achieved smoother roughness compared to this experiment by lower power (50 W). Figure 7 shows the contact angle between a liquid and the thin film surface. The measurement of contact angle often correlates with properties such as adhesion, surface energy and wetting of material. Small water droplet was localized to avoid water surface flattening caused by gravitational force [25]. The thin films show angle value $\theta=57.50^\circ (< 90^\circ)$ that means the sample has high surface-energy (metal-like) [26].

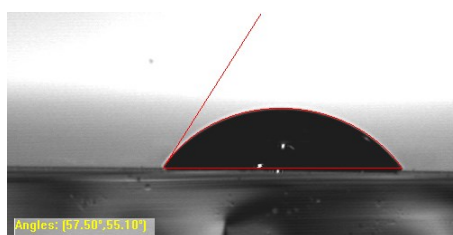


Figure 7. Contact angle of SrSnO_3 film surface

3.2. Electrical conductivity

Electrical conductivity plays an essential role in the electronic application of a semiconductor thin film. The resistivity of SrSnO_3 thin film was measured using a four-point probe and resulted in electrical resistivity of $12.4 \times 10^{-3} \Omega\text{-cm}$, which equivalent to the conductivity of $8.33 \times 10^2 \text{ S/cm}$. The electrical conductivity of an RF sputtered SrSnO_3 thin film is the similar order of magnitude with reported the metal-doped SrSnO_3 thin films of stibium-, neodymium-, and tantalum-doped SrSnO_3 , which the values are $0.1 \times 10^{-5} \Omega\text{-cm}$, $23 \times 10^{-3} \Omega\text{-cm}$, $21 \times 10^{-3} \Omega\text{-cm}$ and $3.33 \times 10^{-3} \Omega\text{-cm}$, respectively [5]. The uniform of grain size and boundary observed in the thin films resulted in the minimum electrical resistivity, thus the structure of the films affected the electrical properties.

4. CONCLUSION

In conclusion, the RF magnetron sputtering technique produce the SrSnO_3 thin film with a thickness of 311 nm and even thickness spreads all over ITO coated glass surface. The XRD patterns showed the sharp curve of (002) reflection peak depicts small FWHM value of 0.47°. Its structure was orthorhombic by finding their different lattice values as mentioned, $a=5.7040 \text{ \AA}$, $b=8.06 \text{ \AA}$, $c=5.7080 \text{ \AA}$ or $a \neq b \neq c$ and $\alpha = \beta = \gamma = 90^\circ$, perpendicular each other. Based on surface observation, it was classified as uniform surface, and its roughness (R_a) value is 2.25 nm. The R_a could achieve smoother value by lowering the RF power in the sputtering process. In the contact angle measurement, high surface energy was obtained on the thin film because the angle is less than 90° , which indicates SrSnO_3 film is a metal-like type and can be functioned with organic material in a heterjunction type structure. The electrical resistivity of $12.4 \times 10^{-3} \Omega\text{-cm}$ for the thin film of SrSnO_3 that obtained is comparable to that of lustrous metal-doped SrSnO_3 thin films with the conductivity of $8.33 \times 10^2 \text{ S/cm}$.

ACKNOWLEDGEMENTS

This work is financially supported by Ministry of Higher Education Malaysia under Fundamental Research Grant Scheme (FRGS/1/2018/TK10/UTHM/03/7) fund and Universiti Malaysia Sabah Research Grant Scheme (SBK0345-2017).

REFERENCE

- [1] M. Ahmadi, T. Wu, and B. Hu, "A review on organic-inorganic halide perovskite photodetectors: device engineering and fundamental physics," *Adv. Mater.*, vol. 29, no. 41, Sep. 2017, doi: 10.1002/adma.201605242.
- [2] H. Wang and D. H. Kim, "Perovskite-based photodetectors: materials and devices," *Chem. Soc. Rev.*, vol. 46, pp. 5204-5236, 2017, doi: 10.1039/C6CS00896H.
- [3] F. Di Giacomo, A. Fakhruddin, R. Jose, and T. M. Brown, "Progress, challenges and perspectives in flexible perovskite solar cells," *R. Soc. Chem.*, pp. 1-26, Sep. 2016, doi: 10.1039/C6EE01137C.
- [4] Y. Yang, H. T. Dai, Feng Yang, and Yating Zhang, "All-Perovskite Photodetector with Fast Response," *Nanoscale Res. Lett.*, vol. 14, Dec. 2019, doi: 10.1186/s11671-019-3082-z.
- [5] A. B. A. Rahman, M. S. Sarjadi, A. Alias, and M. A. Ibrahim³, "Fabrication of Stannate Perovskite Structure as Optoelectronics Material : An Overview Fabrication of Stannate Perovskite Optoelectronics Material : An Overview Structure as," *J. Phys. Conf. Ser.*, vol. 1358, Nov. 2019, doi: 10.1088/1742-6596/1358/1/012043.
- [6] Chen and N. Umezawa, "Sensitization of Perovskite Strontium Stannate SrSnO₃ towards Visible-Light Absorption by Doping," *Int. J. Photoenergy*, pp. 3-6, Aug. 2014, doi: 10.1155/2014/643532.
- [7] M. Faisal, F. A. Harraz, A. A. Ismail, M. A. Alsaiani, and S. A. Al-sayari, "Novel synthesis of Polyaniline/SrSnO₃ nanocomposites with enhanced photocatalytic activity," *Ceram. Int.*, vol. 45, no. 16, pp. 20484-20492, Nov. 2019, doi: 10.1016/j.ceramint.2019.07.027.
- [8] G. Venkatesh, M. Geerthana, S. Prabhu, R. Ramesh, and K. M. Prabu, "Optik Enhanced photocatalytic activity of reduced graphene oxide/SrSnO₃ nanocomposite for aqueous organic pollutant degradation," *Opt.-Int. J. Light Electron Opt.*, vol. 206, no. December 2019, pp. 164055, 2020.
- [9] E. Moreira, J. M. Henriques, D. L. Azevedo, E. W. S. Caetano, V. N. Freire, and E. L. Albuquerque, "Structural , optoelectronic , infrared and Raman spectra of orthorhombic SrSnO₃ from DFT calculations," *J. Solid State Chem.*, vol. 184, no. 4, pp. 921-928, Apr. 2011, doi: 10.1016/j.jssc.2011.02.009.
- [10] Q. Liu, J. Dai, X. Zhang, G. Zhu, Z. Liu, and G. Ding, "Perovskite-type transparent and conductive oxide films : Sb- and Nd-doped SrSnO₃," *Thin Solid Films*, vol. 519, no. 18, pp. 6059-6063, Jul. 2011, doi: 10.1016/j.tsf.2011.03.038.
- [11] M. A. Green, K. Prassides, P. Day, and D. A. Neumann, "Structure of the n=2 and n= member of the Ruddlesden-Popper SrSnO₁₁ n 3n11," *Int. J. Inorg. Mater.* 2, vol. 2, pp. 35-41, 2000.
- [12] K. P. Ong, X. Fan, A. Subedi, M. B. Sullivan, D. J. Singh, and D. J. Singh, "Transparent conducting properties of SrSnO₃ and ZnSnO₃," *APL Mater.*, vol. 3, no. 6, pp. 062505, Jun. 2016, 10.1016/j.tsf.2011.03.038.
- [13] M. A. Riza, S. Sepeai, N. A. Ludin, M. A. M. Teridi, and M. A. Ibrahim, "Synthesis and Characterization Of SrSnO₃ Using Different Synthesis Methods," *Malaysian J. Anal. Sci.*, vol. 23, no. 1, pp. 100-108, 2019, doi: 10.17576/mjas-2019-2301-12.
- [14] H. Wakana, *et al.*, "Examination of deposition conditions for SrSnO₃ insulating layer for single flux quantum circuits," *Phys. C*, vol. 431, pp. 1495-1501, Oct. 2005, doi: 10.1016/j.physc.2005.01.074.
- [15] W. Gao and Z. Li, "ZnO thin films produced by magnetron sputtering," *Ceram. Int.*, vol. 30, no. 7, pp. 1155-1159, 2004, doi: 10.1016/j.ceramint.2003.12.197.
- [16] M. Park, W. Lee, J. G. Lee, and C. Lee, "A Comparison of the Mechanical Properties of RF- and DC- sputter-deposited Cr Thin Films," *Mater. Sci. Forum*, vol. 546, pp. 1695-1698, May 2007, doi: 10.4028/www.scientific.net/MSF.546-549.1695.
- [17] A. I. Journal, Y. Chen, and Y. Shen, "Growth and dielectric characterizations of zinc stannate thin films deposited by RF magnetron sputtering," *Integr. Ferroelectr.*, vol. 192, no. 1, pp. 80-87, 2019, doi: 10.1080/10584587.2018.1522212.
- [18] B. Alshehri, "Design , fabrication and characterization of III-nitrides-based photodiodes : application to high-speed devices," *HAL archives-ouvertes*, 2017.
- [19] A. Rita, F. Alves, A. De Meireles, and E. Longo, "Chemistry SrSnO₃ perovskite obtained by the modified Pechini method-Insights about its photocatalytic activity," *J. Photochem. Photobiol. A*, vol. 369, pp. 181-188, 2019.
- [20] A. Ahmed, M. N. Siddique, U. Alam, T. Ali, and P. Tripathi, "Applied Surface Science Improved photocatalytic activity of Sr doped SnO₂ nanoparticles : A role of oxygen vacancy," *Appl. Surf. Sci. J.*, vol. 463, pp. 976-985, Aug. 2019.
- [21] A. Perron, O. Politano, and V. Vignal, "Grain size , stress and surface roughness," *Surf. Interface Anal.*, vol. 40, no. 3, pp. 518-521, Mar. 2008, doi: 10.1002/sia.2849.
- [22] A. Alghunaim, S. Kirdponpattara, and B. Z. Newby, "Techniques for determining contact angle and wettability of powders," *Powder Technol.*, vol. 287, pp. 201-215, Jan. 2016, doi: 10.1016/j.powtec.2015.10.002.
- [23] A. Ismail, G. B. Kumar, K. A. Mohamad, M. Shahril Osman, F. Pien Chee, Ismail Saad, "Correlation study of structural and optical properties of ZnO / PTAA hybrid heterojunction layer correlation study of structural and optical properties of ZnO / PTAA hybrid heterojunction layer," *J. Phys. Conf. Ser.*, vol. 1358, 2019.
- [24] Y. Zhao, H. Wang, Z. Wang, Fan Yang, "Sputtering power induced physical property variation of nickel oxide films by radio frequency magnetron sputtering," *Mater. Res.*, vol. 21, no. 2, pp. 7-10, 2018, doi: 10.1590/1980-5373-mr-2017-0836.

- [25] S. P. Sakti, Rizal Y. Aji, Layli Amaliya, Masruroh, "Low-cost contact angle measurement system for QCM sensor low-cost contact angle measurement system for QCM sensor," *TELKOMNIKA Telecommunication Computing Electronics and Control*, vol. 15, no. 2, pp. 560-569, Jun. 2017, doi: 10.12928/TELKOMNIKA.v15i2.4981.
- [26] M. C. F. Alves, S. C. Souza, E. C. Paris, S. J. G. Gomes, and L. R. M., "Thermal analysis applied in the crystallization study of SrSnO₃," *Therm. Anal Calorim*, vol. 97, pp. 179-183, 2009.

BIOGRAPHIES OF AUTHORS



Yusmar Palapa Wijaya He graduated with his bachelor (S.Si) in Physics from University Gadjah Mada, Yogyakarta in 2001 and received his master (M.T) from Electronics and Electrical Engineering from University Indonesia, Jakarta and master of science engineering (M.Sc.Eng) from Univeriste Bretagne Occidentale, France in 2011. He joined Electronics Engineering Department of Polytechnic Caltex Riau, Pekanbaru, Indonesia since 2002 and currently as PhD student and Research Assistant at MiNT-SRC and Faculty Electrical and Electronics Engineering University Tun Hussein Onn Malaysia.



Khairul Anuar Mohamad received the BEng in Electronics from University of Electro-communications, Tokyo, Japan in 2001 and the MSc degree in Microelectronics from University of Newcastle upon Tyne, UK in 2004. He received the Doctor of Engineering (Dr.Eng) from Muroran Institute of Technology, Hokkaido, Japan in 2011. He joined Universiti Malaysia Sabag since 2002 and was promoted to Senior Lecturer position in 2011. He also a member of IEEE and IET and a graduate member of Board of Engineer Malaysia (BEM) since 2008. Currently, he is working at Universiti Tun Hussein Onn Malaysia starting from 2017 and appointed as a principal researcher at Microelectronic and Nanotechnology-Shamsuddin Research Center (MiNT-SRC) in 2019. His research interests lie in the area of organic semiconductor thin films and devices and green technology.



Abu Bakar Abd Rahman is a Lecturer in the Faculty of Science and Natural Resources at the Universiti Malaysia Sabah under Industrial Physics programme. He has been appointed as a faculty member since 2015. He completed his MPhil at the University of Southampton in 2010. For undergraduate, he completed it at Universiti Kebangsaan Malaysia in 2000. His background is in Electronics Engineering. His research interests lie in the area of Microelectronics, Semiconductor, Material Science and Solar energy.



Afishah Alias received her B. Eng (Hons) in Electronics Engineering from University of Electro-communications, Tokyo, Japan in 2001 and MSc from University Malaysia Sabah (UMS) specializing in Physics in 2008. In 2011, she received her Doctorate from Muroran Institute of Technology, Hokkaido, Japan specializing in Transparent Conductive Oxide. She has been a full-time lecturer in University Malaysia Sabah (UMS) since 2006 and is promoted as a Senior Lecturer in 2011. She is lecturing in the area of Physics and Electronics. Currently, she is working at Universiti Tun Hussein Onn Malaysia starting since 2017.



Mohammad Syahmi Nordin, He received B.Sc (Physics with Electronics) and M.Sc (Physics) degrees from Universiti Malaysia Sabah in 2005 and 2008 respectively. He obtained his PhD (Applied Physics) in 2018, which focusing on dilute nitride heterostructure devices for the optoelectronic application. His developed device has been patterned as the first resonance cavity enhanced photodetector with internal gain. He is presently working as Senior Research Officer in the School of Computer Science and Electronic Engineering at the University of Essex. His research currently engaged (but not limited to) in the field of semiconductor materials, optoelectronic and biomolecular devices, electronic system engineering and artificial intelligence.